Microseismic Monitoring: Insights from Moment Tensor Inversion

Farshid Forouhideh and David W. Eaton

ABSTRACT

This paper reviews the mathematical tools used for describing microseismic source mechanisms. In addition, based on analysis of synthetic seismograms we develop and evaluate a workflow for inverting source mechanisms (moment tensors). We consider several types of focal mechanisms including double-couple (representative of a slip on a fault) and more complex mechanisms that include tensile forces. Our inversion strategy uses a least-square approach that attempts to fit P- and S-wave amplitudes measured using multicomponent borehole geophone array. An important final step in the inversion process is decomposition of the recovered moment tensor into isotropic, compensated linear vector dipole (CLVD) and double-couple components. These three end member focal mechanisms provide the basis for describing most common classes of microseismic events. Our preliminary inversion tests for noise-free synthetic data suggest that the isotropic component is likely to be the least well-resolved parameter.

INTRODUCTION

With new developments in unconventional gas and the challenging geologic sequestration of carbon dioxide, microseismic monitoring is receiving more and more attention. Operators of frac treatments employ microseismic monitoring in order to define treatment parameters and optimize well spacing. In sequestration projects, microseismic monitoring could shed light on the stress regime and integrity of the reservoir.

Although microseismic monitoring has been extensively used by the mining and geothermal industries, its application in the oil and gas industry is relatively new. Existing tools for analysis of microseismic data have their roots in earthquake seismology. These tools are undergoing development and adaptation by the service industry, but improvements and a better understanding of these techniques will require new research.

One of the important aspects of microseismic monitoring is to delineate the source mechanism of the microseismic events. The common approach to this problem in earthquake seismology is to perform inversion on moment tensors derived from the seismograms recorded by seismic stations. In this report, we have addressed this problem through performing synthetic modeling study, which will be used as the foundation for the next phase of this research project. The main objectives of this report are as following:

1. Brief description of the seismic moment tensor, and inversion and decomposition of the moment tensor ;

2. Forward modeling for a double-couple (DC) source and a combo source with 20% isotropic component, 50% double-couple component and 30% compensated linear vector dipole component;

3. Inversion results for the above cases;

4. Decomposition of the inverted moment tensor of the combo source.

SEISMIC SOURCES AND MOMENT TENSORS

The size of earthquakes is measured from the amplitude of the motion recorded on seismograms. Earthquake seismologists usually express the size of earthquakes in terms of their magnitudes or seismic moments. The former, which is a dimensionless number, is measured in various ways including the body wave magnitude m_b, surface wave magnitude M_s and moment magnitude M_w (for a more detailed discussion on seismic magnitude, see Eaton, 2008). The latter that has dimensions of energy N-m or dyn-cm is the scalar measure of an earthquake rupture size related to the leverage of forces across the area where the fault slips and is expressed by the following formula

$$M_0 = \mu DA, \tag{1}$$

where μ is the shear modulus, D is the average co-seismic displacement and A is the fault area. The scalar seismic moment M_0 is related to the moment magnitude M_w through the equation

$$M_w = \frac{2}{3}\log_{10}(M_0) - 10.7 \ . \tag{2}$$

Seismologists tend to delineate the source mechanism through relating the observed seismic waves to the parameters that best describe the source. In forward modeling problems the theoretical seismic displacements are determined from source models, whereas in inverse problems parameters of source models are derived from observed wave displacements (International Handbook of Earthquake and Engineering Seismology, pp 94). In both problems, the very first step is to define the seismic source by a mechanical model, which represents the physics behind the fracture in the Earth's crust.

In 1923, Nakano presented the first mathematical formulation of the earthquake mechanism. Using the point source approximation, which is valid if the distance between the source and recivers is larger than the seismic source dimensions and wavelengths, Nakano described the source by a system of body forces acting at a point and since these forces are indicating the fracture phenomenon, they are called equivalent forces. It is well-established that most seismic sources can be modeled by force couples (Figure 1). A force couple is composed of two forces acting together. Two basic couples are shown in Fig.1. The couple M_{xy} consists of two forces of magnitude f , separated by a distance d along the y axis, which act in opposite ($\pm x$) directions. The other type is so-called *vector dipole*, which consists of forces with offset in the direction of the force. M_{xx} is composed of two forces of magnitude f acting in the $\pm x$ direction, separated by d along the x axis. The magnitude of both couples is fd and the difference between the two is that the second couple does not exert any torque (Stein and Wysession, 2003).

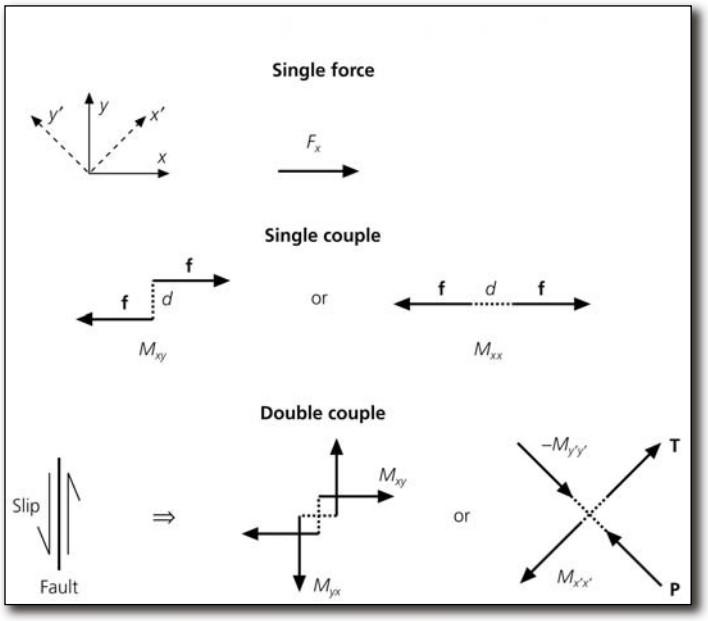

FIG. 1. Schematic description of equivalent body forces. Slip on a fault can be described by the superposition of either couples like M_{xy} and M_{yx} or dipoles like $M_{x'x'}$ and $-M_{y'y'}$ (Stein and Wysession, 2003).

To obtain a general description capable of representing various seismic sources, the force couples of different orientations are combined into a tensor, known as *seismic moment tensor.* The seismic moment tensor was proposed by Gilbert in 1970. The tensor depends on the fault orientation and the source strength and characterizes all information about the source (Stein and Wysession, 2003). The moment tensor and the nine generalized couples are demonstrated in Eqn. 3 and Fig. 2, respectively.

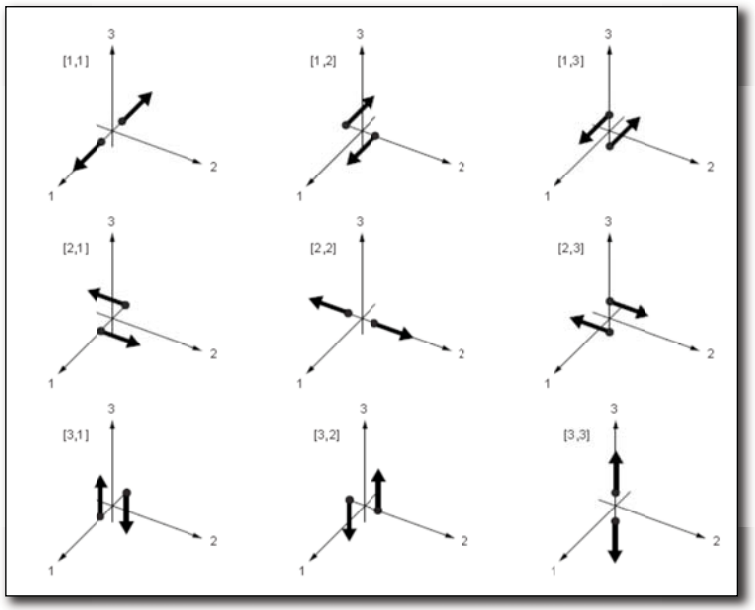

FIG. 2. The nine generalized couples of the seismic moment tensor. Modified after Aki and Richards (1980).

$$M = M_0 \begin{bmatrix} M_{11} & M_{12} & M_{13} \\ M_{21} & M_{22} & M_{23} \\ M_{31} & M_{32} & M_{33} \end{bmatrix}. \quad (3)$$

The moment tensor is symmetric due to the conservation of angular momentum. This reduces the number of independent elements to six in any coordinate system. Any moment tensor can be divided into two parts; double-couple and non-double-couple parts.

Double-couple Sources

Earthquakes that are resulted from a shear or slip on a fault plane may be modeled by a double-couple seismic source. The earthquake shown in Fig. 1 can be represented as

$$M = \begin{bmatrix} 0 & M_0 & 0 \\ M_0 & 0 & 0 \\ 0 & 0 & 0 \end{bmatrix} = M_0 \begin{bmatrix} 0 & 1 & 0 \\ 1 & 0 & 0 \\ 0 & 0 & 0 \end{bmatrix}, \quad (4)$$

where M is the seismic moment tensor and M_0 is the seismic moment scalar. If the fault and slip directions are not well oriented relative to the coordinate system, the seismic moment tensor will be more complicated than Eqn. 4. The moment tensor for a double-couple source in an arbitrary coordinate system appears as following:

$$M_{dc} = M_0 \begin{bmatrix} 2n_x d_x & n_x d_y + n_y d_x & n_x d_z + n_z d_x \\ n_y d_x + n_x d_y & 2n_y d_y & n_y d_z + n_z d_y \\ n_z d_x + n_x d_z & n_z d_y + n_y d_z & 2n_z d_z \end{bmatrix}, \quad (5)$$

where n is the unit normal vector to the fault plane and d is the unit slip vector. The two characteristics of a double-couple moment tensor are that one eigenvalue is zero and that the trace of the tensor is also zero. A non-zero trace corresponds to a volume change (explosion and implosion) and such an isotropic component deos not appear in a pure double-couple (shear) source mechanism (Jost and herrmann, 1989).

Non-double-couple Sources

This group of sources can be categorized into two components. The first is the isotropic component wherein all three diagonal elements of the moment tensor are nonzero and equal. In other words, the isotropic moment tensor (Eqn. 6) is composed of three vector dipoles of three equal and orthogonal force couples, which represents the equivalent body force system for an explosion or implosion (Figure 3; Stein and Wysession, 2003).

$$M_{iso} = \begin{bmatrix} E & 0 & 0 \\ 0 & E & 0 \\ 0 & 0 & E \end{bmatrix}. \quad (6)$$

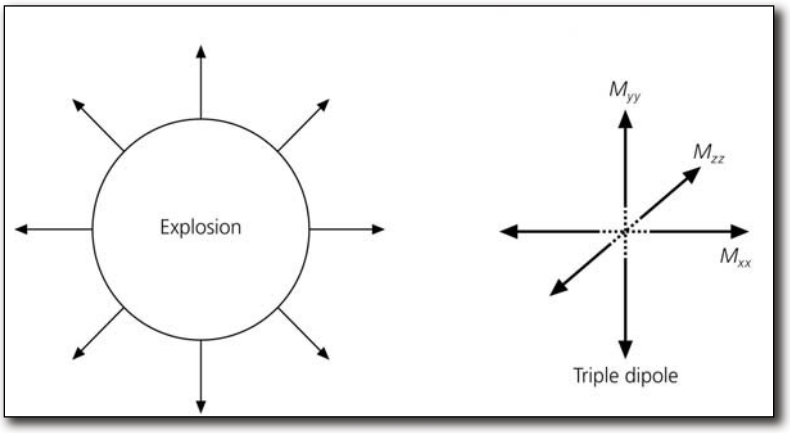

FIG. 3. An explosive source modeled by a triple dipole as an equivalent body force. Modified from (Stein and Wysession, 2003).

The other class of non-double couple seismic sources is the compensated linear vector dipole (CLVD). This category of vector dipoles is compensated for volume change as they are three sets of force dipoles with one dipole -2 times the magnitude of other dipoles. The moment tensor for a CLVD is as following:

$$M_{clvd} = \begin{bmatrix} -\lambda & 0 & 0 \\ 0 & \lambda/2 & 0 \\ 0 & 0 & \lambda/2 \end{bmatrix}. \tag{7}$$

According to Stein and Wysession (2003), there are two primary explanations for CLVD mechanisms. The first is the special case of a magma dike inflating in a volcanic event, which could be modeled as a crack opening under tension. The moment tensor for a crack opening under tension is

$$M_{clvd} = \begin{bmatrix} \lambda & 0 & 0 \\ 0 & \lambda & 0 \\ 0 & 0 & \lambda + 2\mu \end{bmatrix}, \tag{8}$$

where λ and μ are Lame´ elastic constants. As illustrated in Eqn. 8, the trace of the tensor is 3λ + 2μ, which is positive and indicates a volume change. Usually the above tensor is decomposed into two terms:

$$M_{clvd} = \begin{bmatrix} \lambda & 0 & 0 \\ 0 & \lambda & 0 \\ 0 & 0 & \lambda + 2\mu \end{bmatrix} = \begin{bmatrix} E & 0 & 0 \\ 0 & E & 0 \\ 0 & 0 & E \end{bmatrix} + \begin{bmatrix} -2/3\mu & 0 & 0 \\ 0 & -2/3\mu & 0 \\ 0 & 0 & 4/3\mu \end{bmatrix}. \tag{9}$$

On the right hand side, the first term is an isotropic moment tensor whose diagonal components E = λ + 2/3μ are one-third of the trace, and the second term is a CLVD moment tensor. As the inversion of moment tensor for shallow earthquakes cannot

resolve the isotropic component, the seismic wave from such a crack would appear as a CLVD.

The second explanation for CLVD mechanisms is that CLVDs are caused by near-simultaneous earthquakes on close faults of different geometries. Consider the following case that the sum of two double-couple sources results in a CLVD moment tensor:

$$\begin{bmatrix} M_0 & 0 & 0 \\ 0 & 0 & 0 \\ 0 & 0 & -M_0 \end{bmatrix} + \begin{bmatrix} 0 & 0 & 0 \\ 0 & -2M_0 & 0 \\ 0 & 0 & 2M_0 \end{bmatrix} = \begin{bmatrix} M_0 & 0 & 0 \\ 0 & -2M_0 & 0 \\ 0 & 0 & M_0 \end{bmatrix}. \quad (10)$$

One early conclusion from the above example is the non-uniqueness of moment tensor decomposition and that moment tensors can be decomposed in various ways, resulting in different interpretations.

TENSILE EARTHQUAKES

Most earthquakes are caused by shearing or double-couple (DC) mechanisms that do not involve any volume change (isotropic or vector dipole components). In some rare cases, non-double-couple mechanisms represent specific sources such as earthquakes caused by magma intrusion or volume change in mining processes (Vavryčuk, 2001).

In the non-double-couple category, a large number of earthquakes are events with tensile faulting or with combined tensile and shear faulting (Vavryčuk, 2001), which are a good representation of microseismic sources that include volume change. A tensile earthquake is characterized by a slip vector pointing toward an arbitrary direction that does not necessarily lie within the fault plane (Figure 4). As the slip vector deviates from the fault, it causes opening or closing of the fault and thus, it may cause volume change.

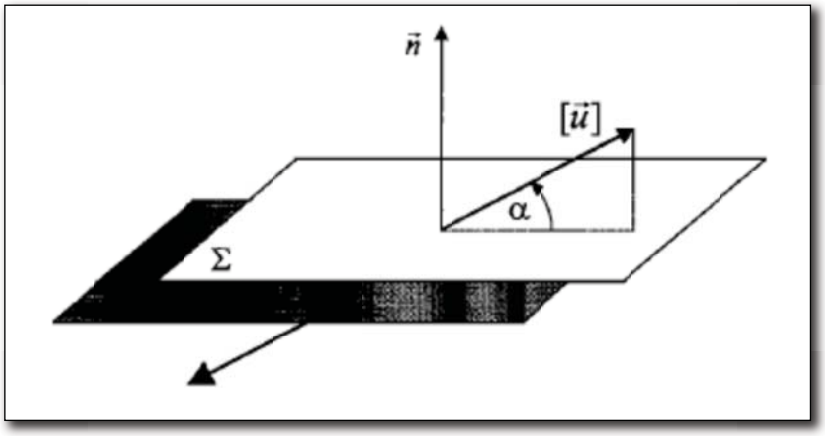

FIG. 4. A model for a tensile earthquake. Σ is the fault plane, $\boldsymbol{n}$ is the nromal to the fault, $\boldsymbol{[u]}$ is the slip vector at the fault and α is the inclination angle from the fault plane (Vavryčuk, 2001).

MOMENT TENSOR INVERSION

Moment tensor and P- and S-waves displacement

Before discussing the inversion of moment tensors for microseismic events, we briefly review the fundamental connection between the source moment tensor and the far-field ground displacement. According to Aki and Richards (1980), the far-field displacement for P- and S-waves traveling in a homogenous elastic space can be described as:

$$U_{k(P|S)}(r,\theta,\phi,t) = \left[\frac{1}{4\pi\rho c^3}\right]\left[\frac{\gamma_k}{r}\right]R_{(P|S)}(\theta,\phi,i,j)\,\dot{M}_{ij}(t), \tag{11}$$

where U_k is the kth component of ground displacement for either P- or S- waves, r is the source-receiver distance, θ and ϕ are the spherical coordinate angles related to the source-receiver take-off and azimuth angles, t is the time in seismogram after a wave's first-arrival time, ρ is density, c is either P- or S-wave velocity, γ_k is the direction cosine between the direction of maximum wave amplitude and the particular displacement component, $R_{(P|S)}$ is the radiation pattern factor for P- and S- waves for each moment tensor component (i or j), and $M_{ij}(t)$ is the moment tensor rate function (MTRF). By integrating Eqn. 11 over the source duration, τ, the following equation is obtained:

$$d_{k(P|S)}(\theta,\phi) = \int\int_{\tau}\dot{U}_{k(P|S)}(r,\theta,\phi,t) = \left[\frac{1}{4\pi\rho c^3}\right]\left[\frac{\gamma_k}{r}\right]R_{(P|S)}(\theta,\phi,i,j)M_{ij}(t), \tag{12}$$

in which, the observed data, $d_{k(P|S)}(\theta,\phi)$, have a direct linear connection to the source decsription, provided by components of the moment tensor, M_{ij}. Therefore, the inversion of the data for source geometry is linear (Nolen-Hoeksema and Ruff, 2001).

By using the representation theorem for seismic sources (Aki and Richards, 1980), Eqn. 12 will take the following form

$$d_n(x,t) = \int_{-\infty}^{\infty}\int_{V} G_{nk}(x,t;r,\bar{t})\,f_k(r,\bar{t})\,dV(r)\,d\bar{t}, \tag{13}$$

where d_n is the observed displacement at an arbitrary position x at the time t due to a distribution of equivalent body force densities f_k, G_{nk} are the components of the Green's functions containing the propagation effects and V is the source volume where f_k are non-zeros (Jost and Herrmann, 1989).

The Green's functions can be expanded into a Taylor series assuming that they vary smoothly within the source volume in the range of moderate frequencies. The Taylor series expansion of the components of the Green's functions around the centroid $r = \varepsilon$ is

$$G_{nk}(x,t;r,\bar{t}) = \sum_{m=0}^{\infty}\frac{1}{m!}(r_{j1}-\varepsilon_{j1})...(r_{jm}-\varepsilon_{jm})G_{nk,j1...jm}(x,t;\varepsilon,\bar{t}), \tag{14}$$

in which the comma between the indices represents partial derivative with respect to the coordinates after the comma. By neglecting the higher order terms in the taylor series, Eqn. 13 becomes

$$d_n(x,t) = M_{kj}[G_{nk,j} * s(\bar{t})], \tag{15}$$

where M_{kj} are constants representing the components of the second order seismic moment tensor M, usually termed the moment tensor and $s(t)$is the source time function (Stump and Johnson, 1977). In Eqn. 15, the displacement d_n is a linear function of the moment tensor elements and the terms in the square brackets. If the source time function $s(t)$ is a delta function, then the only term left in the brackets is $G_{nk,j}$, which describes the nine generalized couples (Jost and Herrmann, 1989).

Moment Tensor Inversion

There are various methods for moment tensor inversion depending on the type of waves, body or surface waves. The inversion can be performed in both time and frequency domain. Eqn. 15 can be used in inversion in the time domain (e.g. Gilbert, 1970; Stump and Johnson, 1977; Strelitz, 1978). Instead, if the source time function is not known, inversion is done in frequency domain (e.g. Gilbert, 1973; Dziewonski and Gilbert, 1974; Stump and Johnson, 1977; Romanowicz, 1981). Eqn. 15 in frequency domain is as following:

$$d_n(x,f) = M_{kj}(f)G_{nk,j}(f)\ . \tag{16}$$

Both Equations (15 and 16) can be written in the matrix form:

$$d = G\overline{m}. \tag{17}$$

In the time domain, d is a vector consisting of n sampled values of the observed ground displacement at various arrival times, station and azimuths. G is a $n \times 6$ matrix containing the Green's functions calculated using an appropriate velocity model and $\overline{m}$ is a vector containing the 6 elements of the moment tensor as shown in Eqn. 18:

$$\begin{bmatrix} d1 \\ d2 \\ : \\ dn \end{bmatrix} = \begin{bmatrix} G_{11} & G_{12} & G_{13} & G_{14} & G_{15} & G_{16} \\ : & : & : & : & : & : \\ : & : & : & : & : & : \\ G_{n1} & G_{n2} & G_{n3} & G_{n4} & G_{n5} & G_{n6} \end{bmatrix} \begin{bmatrix} m_1 \\ m_2 \\ : \\ m_6 \end{bmatrix}. \tag{18}$$

As we have more equations (n) than unkowns (6), the above equation is an overdeterimed system of linear equations. In this case, we cannot invert the matrix G as it is not square. Instead, we use the generalized inverse of G to find the best matching moment tensor with the observed seismograms through a least-square scheme (Jost and Herrmann, 1989):

$$m = \left(G^T G\right)^{-1} G^T u. \tag{19}$$

Moment tensor analysis of microseismic events (-2 < M_w > 2) can be tedious due to the reduction in signal-to-noise ratio. This problem could impose some limitations for the application of moment tensor inversion at the reservoir scale. However, methods have been developed that extend moment tensor inversion to small-magnitude events (e.g., Ma and Eaton, 2009).

Moment Tensor of a Tensile Earthquake

Aki and Richards (1980, equation 3.20) describe the seismic moment tensor $\boldsymbol{M}$ of a point source with isotropic behaviour at a fault as

$$M_{kl} = \lambda[u_1]n_1\delta_{kl} + \mu([u_k]n_l + [u_l]n_k), \tag{20}$$

where λ and μ are Lame' constants at the fault, δ_{kl} is the Kronecker delta, $[u]$ is the slip vector and n is the normal of the fault. By assuming $n = (0,0,1)^T$ and $[\mathbf{u}] = u(\cos\alpha, 0, \sin\alpha)^T$, the moment tensor $\boldsymbol{M}$ takes the following form

$$M = u\begin{bmatrix} \lambda\sin\alpha & 0 & \mu\cos\alpha \\ 0 & \lambda\sin\alpha & 0 \\ \mu\cos\alpha & 0 & (\lambda+2\mu)\sin\alpha \end{bmatrix}, \tag{21}$$

where α ranges between -90° and 90° and denotes the inclination of the slip vector from the fault plane. For α > 0°, the source is tensile and for α < 0°, the source is compressive. The inclination angle of zero (α = 0°) defines a pure shear source, while a pure tensile and a pure compression source are indicated by 90° and -90° inclination angle, respectively. As Dufumier and Rivera (1997) suggested, the moment tensor $\boldsymbol{M}$ can be diagonalized in the principal axis system as following:

$$M = u\begin{bmatrix} \lambda\sin\alpha - \mu(1-\sin\alpha) & 0 & 0 \\ 0 & \lambda\sin\alpha & 0 \\ 0 & 0 & \lambda\sin\alpha + \mu(1+\sin\alpha) \end{bmatrix}. \tag{22}$$

The trace of $\boldsymbol{M}$ is $(3\lambda+2\mu)u.\sin\alpha$. From the stability condition presented by Backus (1962), we have $\mu > 0$ and $\lambda/\mu > -2/3$. The term $(3\lambda+2\mu)$ is always positive, so the sign of the tarce of $\boldsymbol{M}$ is positive for tensile sources and negative for compressive sources (Vavryčuk, 2001).

Decomposition of the Moment Tensor

Typically, moment tensor $\boldsymbol{M}$ is decomposd into three components; isotropic (ISO), compensated linear vector dipole (CLVD) and double-couple (DC) components. The decomposition appears as following (Knopoff and Randall, 1970; Jost and Herrmann, 1989):

$$\boldsymbol{M} = \boldsymbol{M}^{ISO} + \boldsymbol{M}^{CLVD} + \boldsymbol{M}^{DC}, \tag{23}$$

where

$$M^{ISO} = \frac{1}{3} tr(M) \begin{bmatrix} 1 & 0 & 0 \\ 0 & 1 & 0 \\ 0 & 0 & 1 \end{bmatrix},$$

$$M^{CLVD} = |\varepsilon| M^{*}_{|Max|} \begin{bmatrix} -1 & 0 & 0 \\ 0 & -1 & 0 \\ 0 & 0 & 2 \end{bmatrix},$$

$$M^{DC} = (1 - 2|\varepsilon|) M^{*}_{|\max|} \begin{bmatrix} -1 & 0 & 0 \\ 0 & 0 & 0 \\ 0 & 0 & 1 \end{bmatrix}.$$

The sum of the ISO and CLVD components is called the non-DC component and the sum of the CLVD and DC components is called the deviatoric moment $\boldsymbol{M}^{*}$. In above equations, parameter ε is a measure of the size of CLVD relative to DC component (Sipkin, 1986; Kuge and Lay, 1994; Julian et. Al, 1998, equation 18) and is defined by

$$\varepsilon = -\frac{M^{*}_{|\min|}}{\left|M^{*}_{|Max|}\right|}, \tag{24}$$

in which $M^{*}_{|\min|}$ and $M^{*}_{|Max|}$ are the minimum and maximum absolute values of the eigenvalues of deviatoric moment $\boldsymbol{M}^{*}$. For a pure CLVD source, ε = ±0.5 and for a pure DC source, ε = 0. Also, ε is positive for tensile sources and negative for compressional sources.

SYNTHETIC MODELING RESULTS

Forward Modeling

We have performed forward modeling for two seismic sources with assumed locations for the source and receiver arrays (Figure 5). The first one is a double-couple source mechanism with a dip of 90°, slip or rake of 0° and strike of 0° and the second one is a source composed of 20% isotropic, 50% double-couple and 30% CLVD components (Combo source) with the same fault parameters as above. The moment tensors for these sources with assumed magnitude -1 are as following:

$$M_{dc} = 1e+21 \times \begin{bmatrix} 0 & 3.5481 & 0 \\ 3.5481 & 0 & 0 \\ 0 & 0 & 0 \end{bmatrix}, \tag{25}$$

$$M_{combo} = 1e+21 \times \begin{bmatrix} 1.7741 & 1.7741 & 0 \\ 1.7741 & -1.4193 & 0 \\ 0 & 0 & 1.7741 \end{bmatrix}. \quad (26)$$

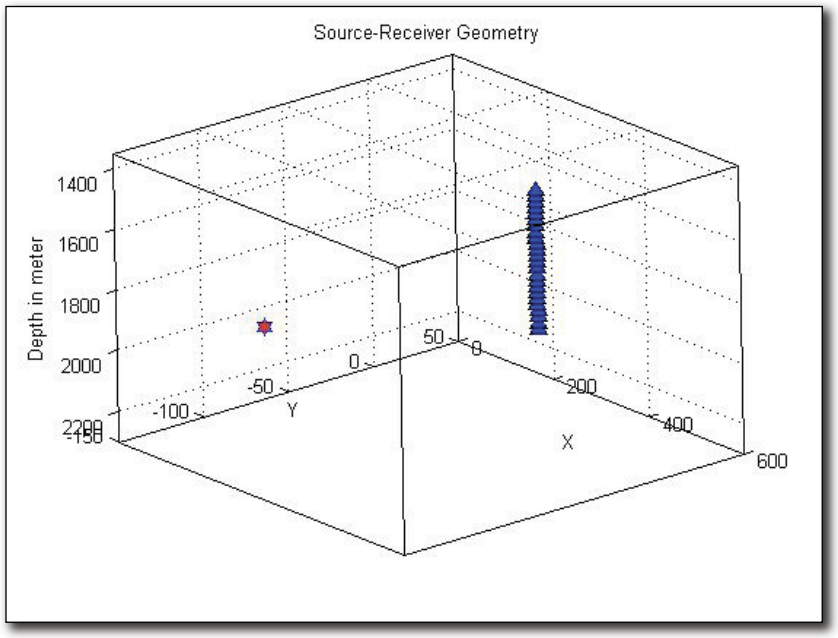

FIG. 5. Assumed source and receiver arrays used in this synthetic modeling.

The focal mechanism (beach ball diagram) and the P-wave radiation pattern for these sources are demonstrated in Fig. 6 through Fig. 9.

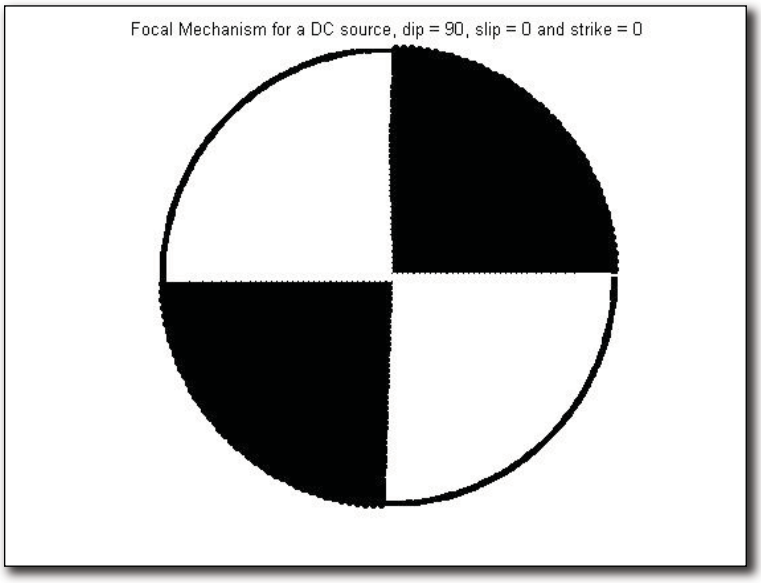

FIG. 6. Focal mechanism for a double-couple source.

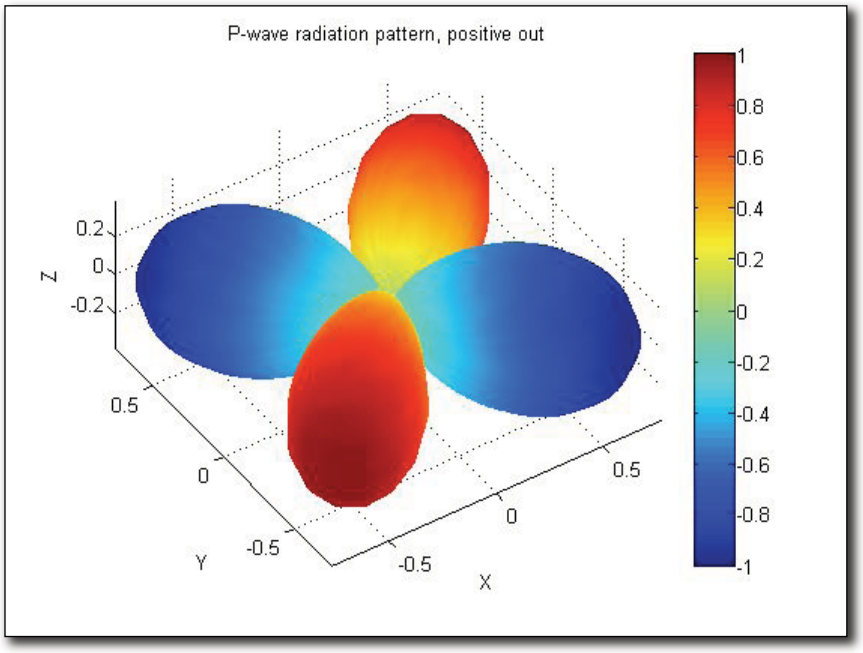

FIG. 7. P-wave radiation pattern for a double-couple source.

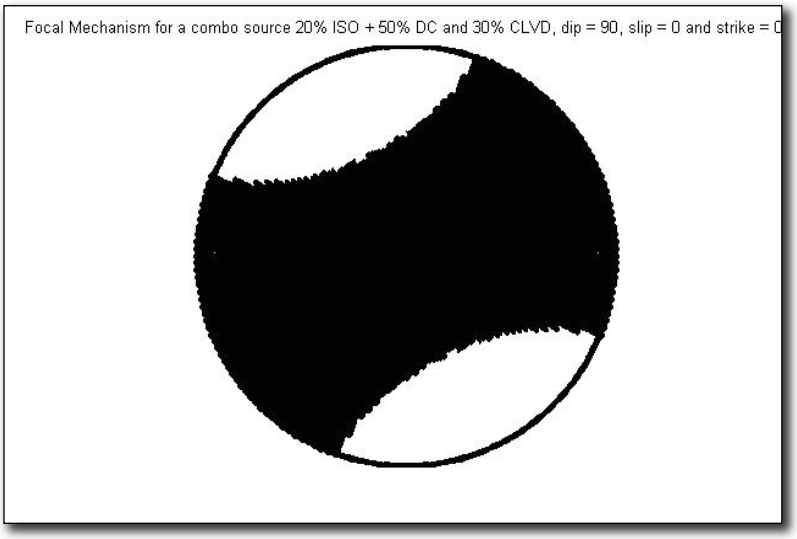

FIG. 8. Focal mechanism for a source with 20% isotropic, 50% double-couple and 30% CLVD components.

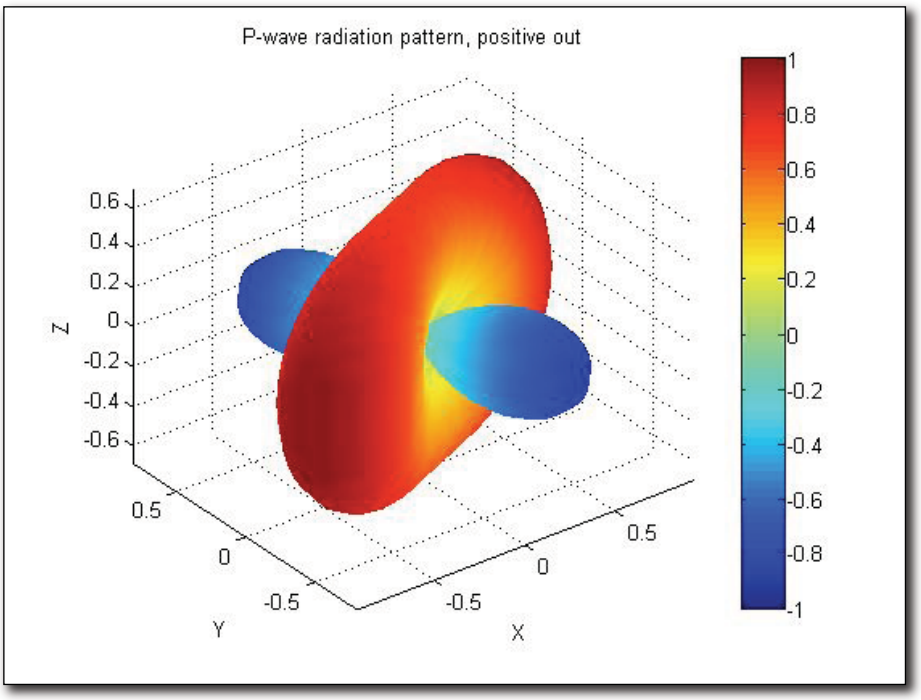

FIG. 9. P-wave radiation pattern for the above combo source.

Using M_{dc}, M_{combo} and Eqn. 12, the synthetic seismograms for the given source were calculated. The seismograms for the DC and Combo sources are shown in the following

figures. The figures show three components of the seismograms 1,2 and 3 that correspond to X, Y and Z directions, respectively.

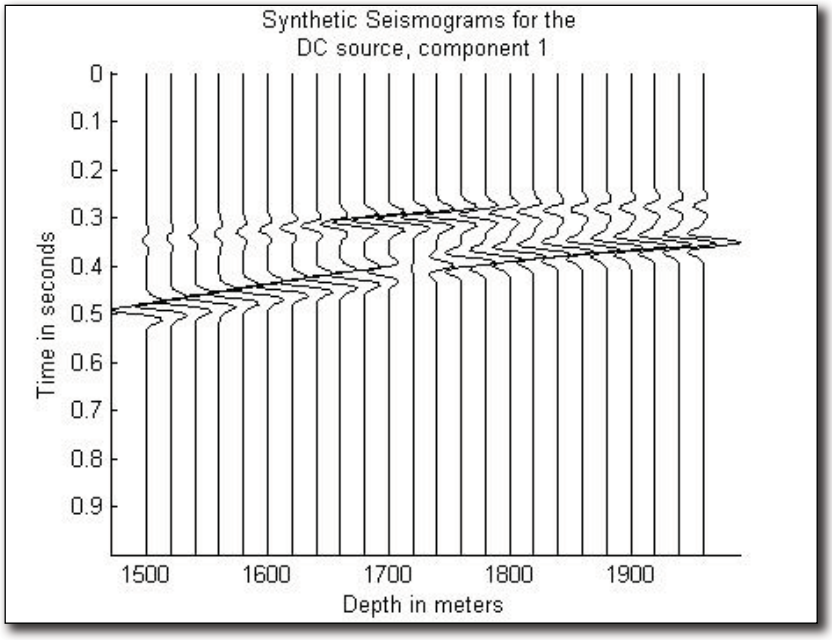

FIG. 10. Synthetic seismograms for the DC source in X direction (Component 1).

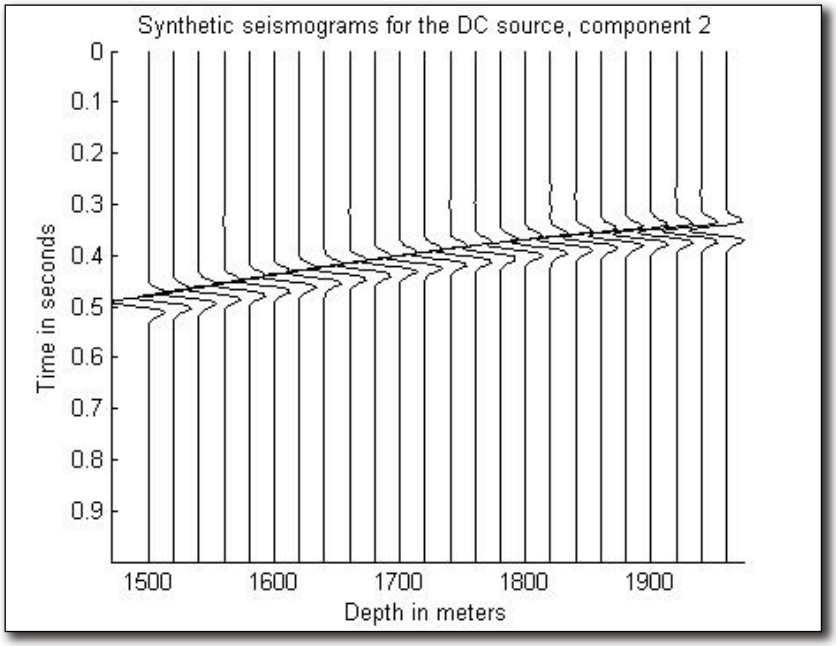

FIG. 11. Synthetic seismograms for the DC source in Y direction (2nd component).

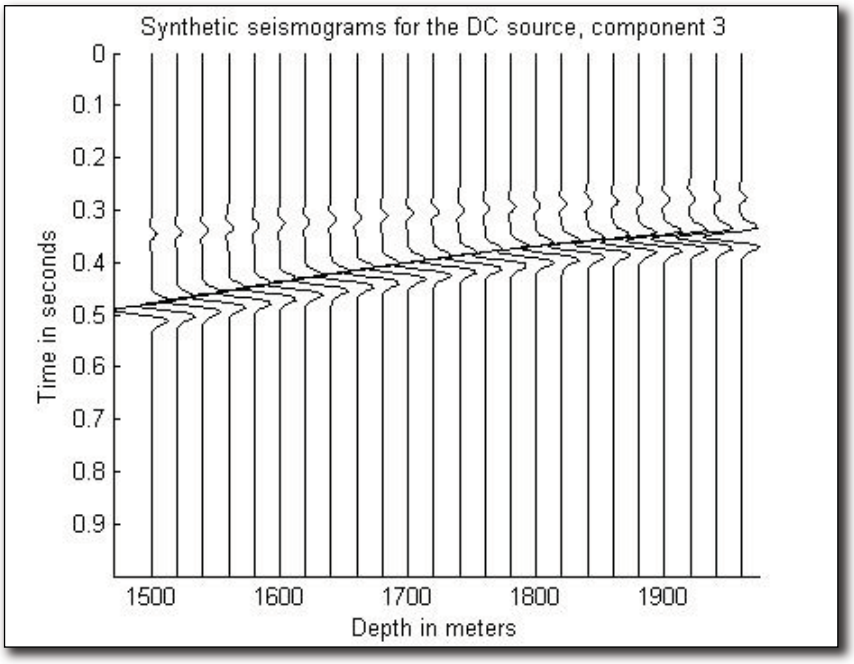

FIG. 12. Synthetic seismograms for the DC source in Z direction (3rd component).

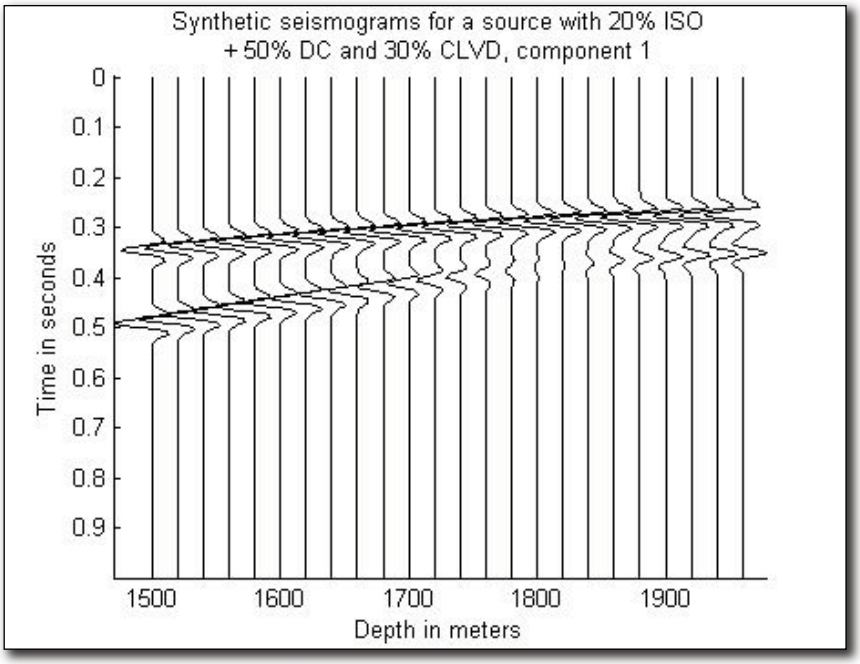

FIG. 13. Synthetic seismograms for the Combo source (1st component).

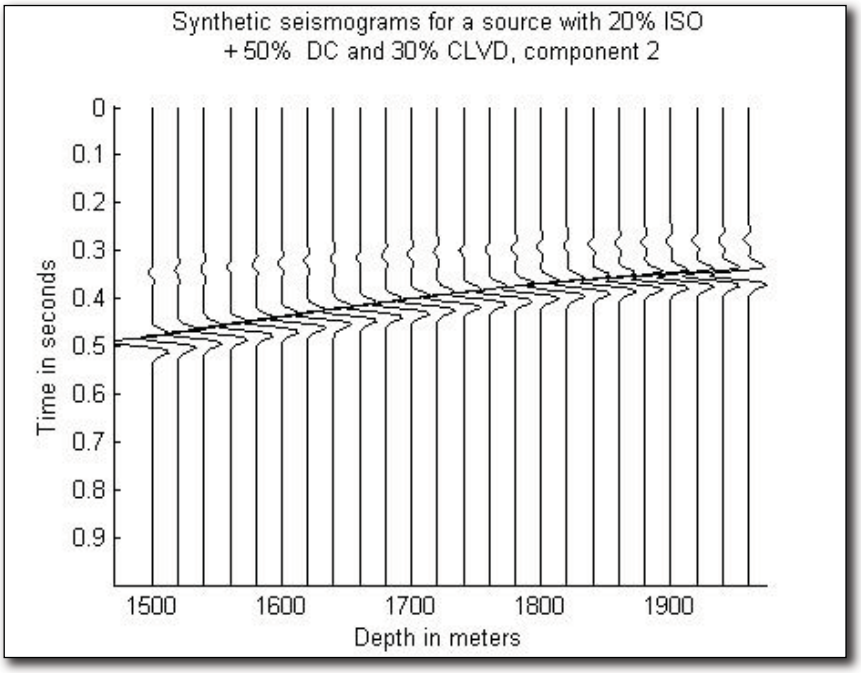

FIG. 14. Synthetic seismograms for the Combo source (2nd component).

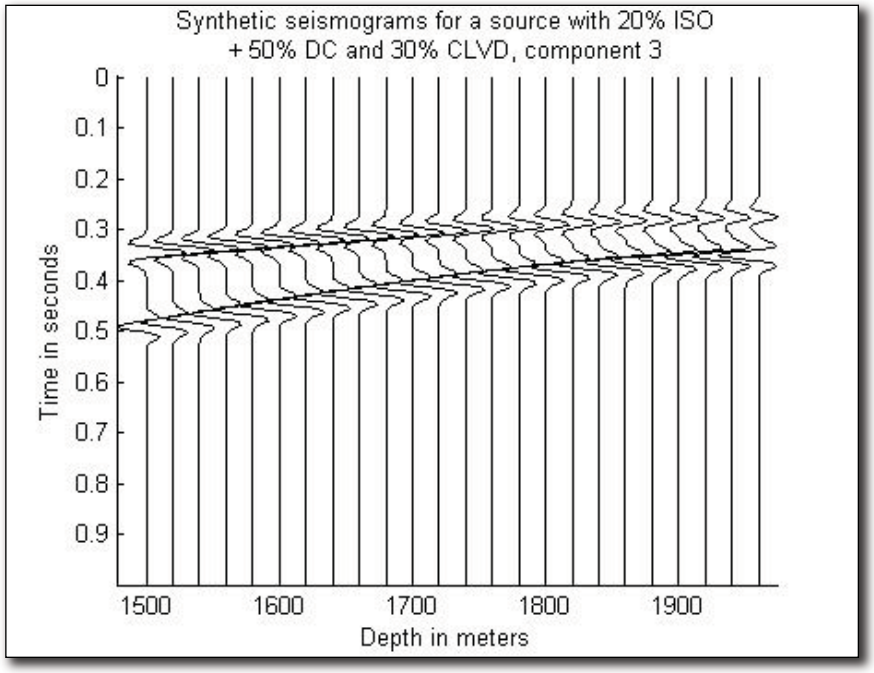

FIG. 15. Synthetic seismograms for the Combo source (3rd component).

Inversion Results and Decomposition of the Inverted Moment Tensor

After performing the forward modeling and obtaining the seismograms for the DC and Combo sources, we inverted the seismograms to acquire the moment tensor for the sources and the assumed source and receiver geometry using a least-square approach. The resulting moment tensors are as following:

$$M_{Inv-dc} = 1e+21 \times \begin{bmatrix} -4.7251 & 9.4066 & 0.6223 \\ 9.4066 & -9.5789 & 4.1920 \\ 0.6223 & 4.1920 & -0.8151 \end{bmatrix}, \quad (27)$$

$$M_{Inv-combo} = 1e+21 \times \begin{bmatrix} 2.2835 & -0.6231 & 0.9191 \\ -0.6231 & 5.7821 & -0.0014 \\ 0.9191 & -0.0014 & 1.5267 \end{bmatrix}. \quad (28)$$

The focal mechanisms for the inverted sources are shown in Fig. 16 and 17. The result of decomposing the $M_{Inv\text{-}combo}$ into isotropic, CLVD and DC components is summarized in Table 1.

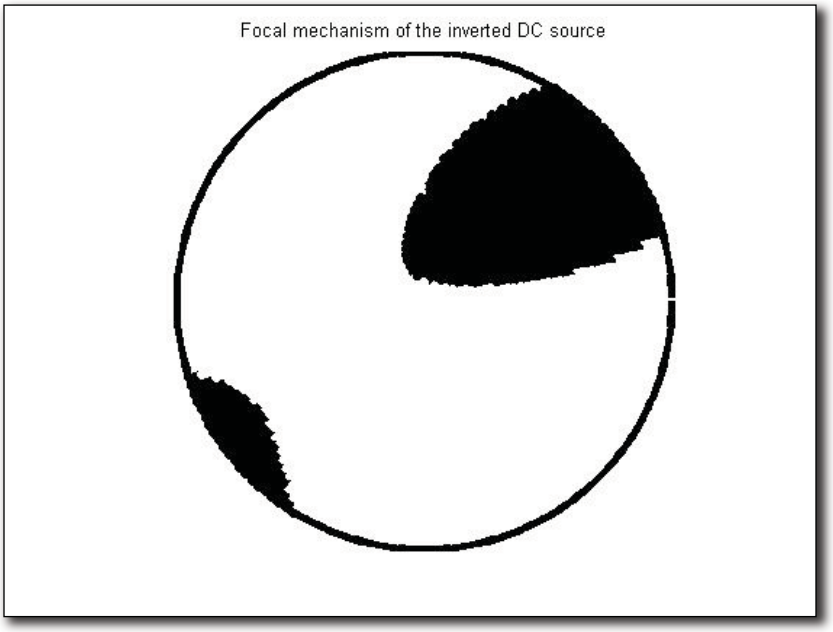

FIG. 16. Focal mechanism corresponding to the inverted moment tensor for the DC source.

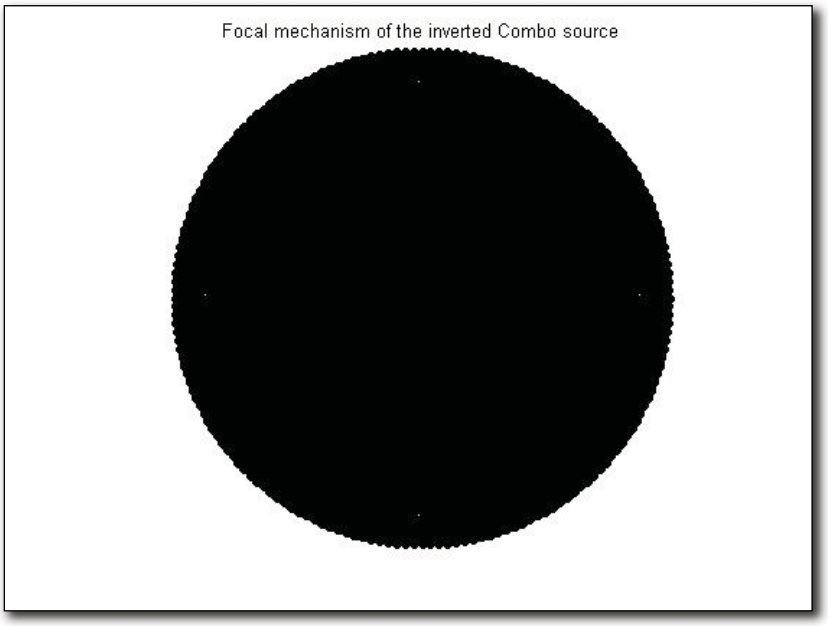

FIG. 17. Focal mechanism corresponding to the inverted moment tensor for the Combo source.

Table. 1. Decomposition of the inverted moment tensor for the Combo source.

Components	Combo FWD Modeling	Combo Inverted
ISO %	20	3.7
CLVD %	30	27.6
DC %	50	68.7

CONCLUSION

Considering that this study is still in progress, our preliminary synthetic modeling and inversion tests suggest the following points that are important to be considered in practical aspects:

1. With a single observation borehole, it is impossible to solve for the full moment tensor elements and even obtaining an accurate inversion result.

2. Moment tensor analysis is a powerful tool in delineating the source parameters mathematically.

3. Decomposition of moment tensor is not unique and various decompositions may lead to different interpretations.

4. The isotropic component is the least well-resolved parameter through moment tensor inversion of data obtained from one single observation well.

REFERENCES

Aki, K., and Richards, P. G., 1980, Quantitative Seismology: Theory and Methods, W. H. Freeman and Co.

Backus, G. E., 1962, Long-wave anisotropy produced by horizontal layering, Journal of Geophysical Research, **66**, 4427-4440.

Dufumier, H., and Rivera, L., 1997, On the resolution of the isotropic component in moment tensor, Geophysical Journal International, **131**, 595-606.

Dziewonski, A. M., and Gilbert, F., 1974, Temporal variation of the seismic moment tensor and the evidence of precursive compression for two deep earthquakes, Nature, **247**, 185-188.

Eaton, D. W., 2008, Microseismic focal mechanism: A tutorial, CREWES Research Report.

Gilbert, F., 1970, Excitation of the normal modes of the Earth by earthquake sources, Geophysical Journal of the Royal Astrophysical Society, **22**, 223-226.

Jost, M. L., and Herrmann, R. B., 1989, A student's guide to and review of moment tensors, Seismological Research Letters, **60**, 2, 37-57.

Julian, B. R., Miller, A. D., and Fougler, G. R., Non-double-couple earthquakes, 1, Theory, Reviews of Geophysics, **36**, 525-549.

Knopoff, L., and Randall, M. J., The compensated linear vector dipole: A possible mechanism for deep earthquakes, Journal of Geophysical Research, **75**, 4957-4963.

Kuge, K, and Lay, T., 1994, Data-dependent non-double-couple components of shallow earthquakes source mechanisms: Effects of waveform instability, Geophysical Research Letters, **21**, 9-12.

Lee, W. H.K., Kanamori, H., Jennings, P. C., and Kisslinger, C., 2002, International Handbook of Earthquake & Engineering Seismology, Academic press Inc.

Ma, S., and Eaton, D. W., 2009, Anatomy of small earthquake swarm in southern Ontario, Canada: Seismological Research Letters, **80**, 214-223.

Nolen-Hoeksema, R. C., and Ruff, L. J., 2001, Moment tensor inversion of microseisms from the B-sand propped hydrofracture, M-site, Colorado: Technophysics, **336**, 163-181.

Romanowics, B., 1981, Depth resolution of earthquakes in central Asia by moment tensor inversion of long-period Rayleigh waves: Effects of phase velocity variations across Eurasia and their calibration, Journal of Geophysical Research, **86**, 5963-5984.

Sipkin, S. A., 1986, Interpretation of non-double-couple earthquake mechanisms derived from moment tensor inversion, Journal of Geophysical Research, **91**, 531-547.

Stein, S., and Wysession, M., 2003, An Introduction to Seismology, Earthquakes, and Earth Structure, Blackwell Publishing.

Strelitz, R. A., 1978, Moment tensor inversions and source models, Geophysical Journal of the Royal Astronomical Society, **52**, 359-364.

Stump, B. W., and Johnson, L. R., 1977, The determination of source properties by the linear inversion of seismograms, Bulletin of Seismological Society of America, **67**, 1489-1502.

Vavryčuk, V., 2001, Inversion for parameters of tensile earthquakes, Journal of Geophysical Research, **106**, 16,339–16,355.